ENERGY LEVELS AND RADIATIVE RATES IN Ga XVII**

F. Hu [1*], Y. Sun [1], Ch. Han [1], M. Mei [1], C. Sang [2], H. Liu [3], Ch. Wang [3]

[1] School of Mathematical and Physical Sciences at Xuzhou University of Technology, Xuzhou 221018, China; e-mail: hufengscu@139.com
[2] College of Science at Lanzhou University of Technology, Lanzhou 730050, China
[3] Research Center of Laser Fusion of the China Academy of Engineering Physics, Mianyang 621900, China

Complete and consistent atomic data, including energy levels, wavelengths, lifetimes and E1, E2, M1, and M2 transition rates, are reported for the low-lying 41 levels of Ga XVII, belonging to the n=3 states ($1s^2 2s^2 2p^6 3s^2 3p^3$, $3s3p^4$, and $3s^2 3p^2 3d$. High-accuracy calculations act as benchmarks for accurate treatments of relativity, electronic correlation, and quantum electrodynamic (QED) effects in multi-valence-electron systems. The calculated energy levels are in excellent agreement with the experimental results and the experimentally compiled energy values of the National Institute for Standards and Technology wherever available. The calculated values, including core-valence correction, are found to be in good agreement with other theoretical and experimental values.

Keywords: *energy level, wavelength, transition rate.*

УРОВНИ ЭНЕРГИИ И СКОРОСТИ ИЗЛУЧЕНИЯ ИОНА Ga XVII

F. Hu [1*], Y. Sun [1], Ch. Han [1], M. Mei [1], C. Sang [2], H. Liu [3], Ch. Wang [3]

УДК 535.14

[1] Школа физико-математических наук Технологического университета Сюйчжоу, Сюйчжоу 221018, Китай; e-mail: hufengscu@139.com
[2] Колледж наук Технологического университета Ланьчжоу, Ланьчжоу 730050, Китай
[3] Китайская академия инженерной физики, Мяньян 621900, Китай

(Поступила 8 августа 2019)

Представлен полный и непротиворечивый набор данных о низколежащих 41 уровнях Ga XVII, принадлежащих состояниям с n = 3 ($(1s^2 2s^2 2p^6 3s^2 3p^3$, $3s^3 p^4$ и $3s^2 3p^2 3d$), в том числе уровни энергии, длины волн, времена жизни и скорости переходов E1, E2, M1 и M2. Высокоточные расчеты могут выступать в качестве эталона при точной трактовке эффектов относительности, электронной корреляции и квантовых электродинамических явлений в многоэлектронных системах. Рассчитанные уровни энергии находятся в хорошем согласии с экспериментальными результатами и данными, представленными Национальным институтом стандартов и технологий. Рассчитанные значения, включая корреляцию ядро—валентность, находятся в хорошем соответствии с другими теоретическими и экспериментальными данными.

Ключевые слова: *уровень энергии, длина волны, скорость перехода.*

Introduction. Radiative transitions of heavy elements play an important role in astrophysics. Studying the abundances of these heavy elements produced by neutron capture processes requires the oscillator strengths of the detected lines [1]. The Ga element was found overabundant in some stars such as HgMn ones and hot white dwarfs [2]. Moreover, Ga ions were used to investigate the plasma temperature in inertial confinement fusion [3]. However, in order to interpret observations or simulate the plasmas, information on some atomic parameters, such as energy levels, wavelengths, and lifetimes, is needed [3]. Therefore, over

** Full text is published in JAS V. 87, No. 6 (http://springer.com/journal/10812) and in electronic version of ZhPS V. 87, No. 6 (http://www.elibrary.ru/title_about.asp?id=7318; sales@elibrary.ru).

a period of time many researches have reported atomic data for a few Ga ions. The general-purpose relativistic atomic structure package (GRASP) was used by Aggarwal to compute the energy levels, radiative rates, and lifetimes of Ga XXII [4]. The multiconfiguration Dirac-Hartree-Fock (MCDHF) and second-order many-body perturbation theory was employed by Li et al. to give the excitation energies, line strengths, wavelengths, and transition rates for Ga XXIII [5]. Large-scale self-consistent MCDHF subsequent relativistic configuration interaction (RCI) calculations were reported by Ekman et al. to obtain the $E1$, $E2$, $M1$, and $M2$ transition rates and associated lifetimes for Ga XIX [6]. But for Ga XVII, only a small number of investigations have been done. The wavelengths and transition rates for magnetic-dipole transitions within the $3s^2 3p^n$ ground configuration of Ga XVII were predicted by Sugar and Kaufman [7]. The multiconfiguration Dirac-Fock technique was used by Huang to represent the theoretical energy levels and transition probabilities for Ga XVII [8]. The oscillator strengths for the dipole-allowed fine-structure $3p^3\ {}^4S^o–3p^2({}^3P)3d\ {}^4P$ transition array of Ga XVII were obtained by Charro et al. using the relativistic quantum defect orbital method [9]. The Ga XVII theoretical calculations were evaluated by Vilkas and Ishikawa on the basis of the relativistic multireference many-body perturbation theory [10].

Träbert conducted a critical assessment of the theoretical calculations of the structure and transition probabilities from an experimenter's view [11]. He pointed out that new computations can match measurement, fill in gaps, and suggest revisions closely with an almost spectroscopic accuracy. These citations of the theoretical work as well as the ones for experimental data are obviously incomplete. These citations were a number of P-like ion calculations, and attention was paid to the trend. So, limited energy levels [8, 10] or transitions [9] were considered, or some selected configurations were discussed [9]. Some results were given as graphs [8]. Yet, there still exist problems such as the definition of terms and strong mixing of configurations, which will be discussed in detail in the next part of this paper.

In this paper, the large-scale MCDHF method is used to calculate the $E1$, $E2$, $M1$, and $M2$ wavelengths, oscillator strengths, transition probabilities, and fine-structure levels for Ga XVII using the new release of the GRASP2K code [12, 13]. Configurations $(1s^2 2s^2 2p^6)3s^2 3p^3$, $3s3p^4$, and $3s^2 3p^2 3d$ are reported in this calculation. Based on our previous work [14–16], in this paper, the valence-valence (VV) and core-valence (CV) correlation effects are considered in a systematic way. Breit interactions and quantum electrodynamics (QED) effects are added. This computational approach enables us to present a consistent and improved data set of all important $E1$, $E2$, $M1$, and $M2$ transitions of the Ga XVII spectra, which are useful for identifying transition lines in further investigations.

Calculation. Recently the MCDHF method has been described in detail by Grant [17]. Meanwhile, different correlations were included into the calculation. The correlation energy is defined as the energy difference between the exact solution of the Dirac equation and the Dirac-Fock (DF) solution. Then the contribution from the correlation can be defined as the energy difference between the solution including the particular correlation under investigation and the DF solution. To classify the correlation, the atomic electrons can be separated in two groups, namely, valence and core electrons [17]. As a result, the correlation between the valence electrons is defined as VV, and the correlation between the valence and core electrons is defined as CV [17].

In our calculations, we generate the CSFs using the active space approach. We do this by exciting electrons from the spectroscopic reference configuration to the orbitals called the active set (AS). The latter is a set of orbitals combining all orbitals except the common for all configuration state functions (CSFs). We increase the AS in a systematic way to ensure the convergence of the atomic parameters under consideration.

A similar calculation procedure was introduced in [14–16]. In our VV method, we set $1s^2 2s^2 2p^6$ as our core electrons in the calculation. Then we considered increasing the principal quantum number n (n = 4–7), and optimized the orbitals AS1, AS2, AS3, and AS4. In the CV model, the core is $1s^2 2s^2 2p^5$; then we optimized the layer by n. We generated the CSFs of the form of $1s^2 2s^2 2p^5 \mathrm{AS}_n$, n = 1–4. The $3s^2 3p^3$, $3p^5$, $3s3p^3 3d$ odd and the $3s3p^4$, $3s^2 3p^3 3d$, $3s3p^2 3d^2$ even configurations were included in this work. The number of CSFs used in the atomic state function expansion for the given angular momentum and parity (J^P) took into account only single-double (SD) excitations.

Results and discussion. Data for the $3s^2 3p^3$, $3s3p^4$, and $3s^2 3p^2 3d$ configurations of Ga XVII are listed in Table 1, where we compare our results with the experimental ones compiled by the National Institute for Standards and Technology (NIST) [18]. The NIST database lists the energies for 11 out of the present 41 excited-levels in Ga XVII. The theoretical results from Vilkas and Ishikawa [10] and the on-line data from ADAMANT (Applicable Data of Many-Electron Atom eNergies and Transitions) [19] are also listed in Table 1. The present results from VV and CV calculations are reported when n = 7.

TABLE 1. Energies (in cm^{-1}) Relative to the Ground State for the Lowest 41 Levels in Ga XVII

Key	Level	VV $n = 7$	CV $n = 7$	Vilkas [10]	ADAMANT [19]	NIST [18]
1	$3s^23p^3\ ^4S_{3/2}$	0	0	0	0	0
2	$3s^23p^3\ ^2D_{3/2}$	53994	53935	52965	54194	52916
3	$3s^23p^3\ ^2D_{5/2}$	68764	68727	67678	68362	67727
4	$3s^23p^3\ ^2P_{1/2}$	106209	106284	104629	105755	104622
5	$3s^23p^3\ ^2P_{3/2}$	130058	130189	128787	128434	128577
6	$3s3p^4\ ^4P_{5/2}$	382980	383352	383398	383642	
7	$3s3p^4\ ^4P_{3/2}$	407744	408201	408284	407843	
8	$3s3p^4\ ^4P_{1/2}$	416308	416788	416782	416369	
9	$3s3p^4\ ^2D_{3/2}$	476386	476286	475747	476778	
10	$3s3p^4\ ^2D_{5/2}$	484526	484501	483979	484495	
11	$3s^23p^23d\ (^3P_2)\ ^2P_{3/2}$	541878	540937	537024	541576	
12	$3s^23p^23d\ (^3P_2)\ ^2P_{1/2}$	548166	547143	540559	548030	
13	$3s^23p^23d\ (^3P_2)\ ^4F_{3/2}$	573649	572898	546106	575234	
14	$3s^23p^23d\ (^3P_2)\ ^4F_{5/2}$	583788	583094	583247	584808	
15	$3s3p^4\ ^2S_{1/2}$	585690	585028	583964	585235	
16	$3s^23p^23d\ (^3P_2)\ ^4F_{7/2}$	599714	599112	599130	600532	
17	$3s^23p^23d\ (^1D_2)\ ^2F_{5/2}$	601240	600582	600407	602430	
18	$3s^23p^23d\ (^1D_2)\ ^2F_{7/2}$	612704	612086	611784	613497	
19	$3s^23p^23d\ (^3P_2)\ ^4D_{1/2}$	614214	613407	613344	614578	
20	$3s^23p^23d\ (^3P_2)\ ^4D_{3/2}$	615252	614432	614458	615825	
21	$3s^23p^23d\ (^3P_2)\ ^4F_{9/2}$	616154	615620	615533	616640	
22	$3s^23p^23d\ (^3P_2)\ ^4D_{5/2}$	626607	625899	625855	627102	
23	$3s^23p^23d\ (^3P_2)\ ^4D_{7/2}$	651110	650594	650298	650949	
24	$3s^23p^23d\ (^1D_2)\ ^2G_{7/2}$	680741	680002	678940	682010	
25	$3s3p^4\ ^2P_{3/2}$	686943	683009	681146	684273	
26	$3s^23p^23d\ (^1D_2)\ ^2G_{9/2}$	690986	690373	689275	691839	
27	$3s^23p^23d\ (^3P_2)\ ^4P_{5/2}$	698014	694325	693860	696495	693419
28	$3s^23p^23d\ (^3P_2)\ ^4P_{3/2}$	706111	702631	702168	704416	701630
29	$3s^23p^23d\ (^3P_2)\ ^4P_{1/2}$	709804	706163	705329	707249	
30	$3s^23p^23d\ (^1S_0)\ ^2D_{3/2}$	719804	718226	716819	717924	
31	$3s3p^4\ ^2P_{1/2}$	722100	718248	717378	720772	
32	$3s^23p^23d\ (^1D_2)\ ^2D_{5/2}$	743687	740912	739991	742909	
33	$3s^23p^23d\ (^1D_2)\ ^2D_{3/2}$	760860	757249	755875	758503	
34	$3s^23p^23d\ (^1S_0)\ ^2D_{5/2}$	764632	763034	761580	765576	
35	$3s^23p^23d\ (^1D_2)\ ^2P_{1/2}$	774958	771645	770397	775331	
36	$3s^23p^23d\ (^3P_2)\ ^2F_{5/2}$	780846	776919	775653	779637	
37	$3s^23p^23d\ (^3P_2)\ ^2F_{7/2}$	796049	792228	790695	794296	789800
38	$3s^23p^23d\ (^1D_2)\ ^2P_{3/2}$	797416	794064	792864	796613	793220
39	$3s^23p^23\mathrm{d}\ (^1D_2)\ ^2S_{1/2}$	801871	798538	796501	799591	
40	$3s^23p^23d\ (^3P_2)\ ^4D_{3/2}$	833567	830206	828484	832962	
41	$3s^23p^23d\ (^3P_2)\ ^4D_{5/2}$	834045	830429	828948	833237	828010

Table 1 demonstrates that for the CV approach the deviation of the theoretical results from the experimental ones is in the range ~1.25–1.92% for the $3s^23p^3$ levels and about ~0.12–0.31% for the $3s^23p^23d$ levels (Fig. 1a), while for the VV approach this deviation is in the range ~1.15–2.03% for the $3s^23p^3$ levels and about ~0.43–0.79% for the $3s^23p^23d$ levels (Fig. 1b). The results from ADAMANT differ from the experimental results by 1.00% for the $3s^23p^3$ levels, and by about 0.50% for the $3s^23p^23d$ levels. The most accurate calculations were carried out by Vilkas and Ishikawa [10], where the difference between the theoretical and experimental results achieved 0.10% for the majority of the excited levels. These calculations can be treated as benchmarks for the experimental results.

In order to give a clear representation of valence electrons, comparisons between MCDHF and Vilkas and Ishikawa [10] are plotted in Figs. 1c,d, where the contribution from core electrons can be found. The dif-

ference between the valence-valence correlation results and the energies from Vilkas and Ishikawa is in the range –396~5865 cm^{-1}, whereas for CV it is –2~2037 cm^{-1}. Also, the contribution from the higher orbital decreases with increase in the principal number n. The contribution from $n = 7$ is only 0.06%. It should be noted that, as follows from Figs. 1c,d, in some cases, due to configuration mixing, the consideration of a larger number of configurations is less correct.

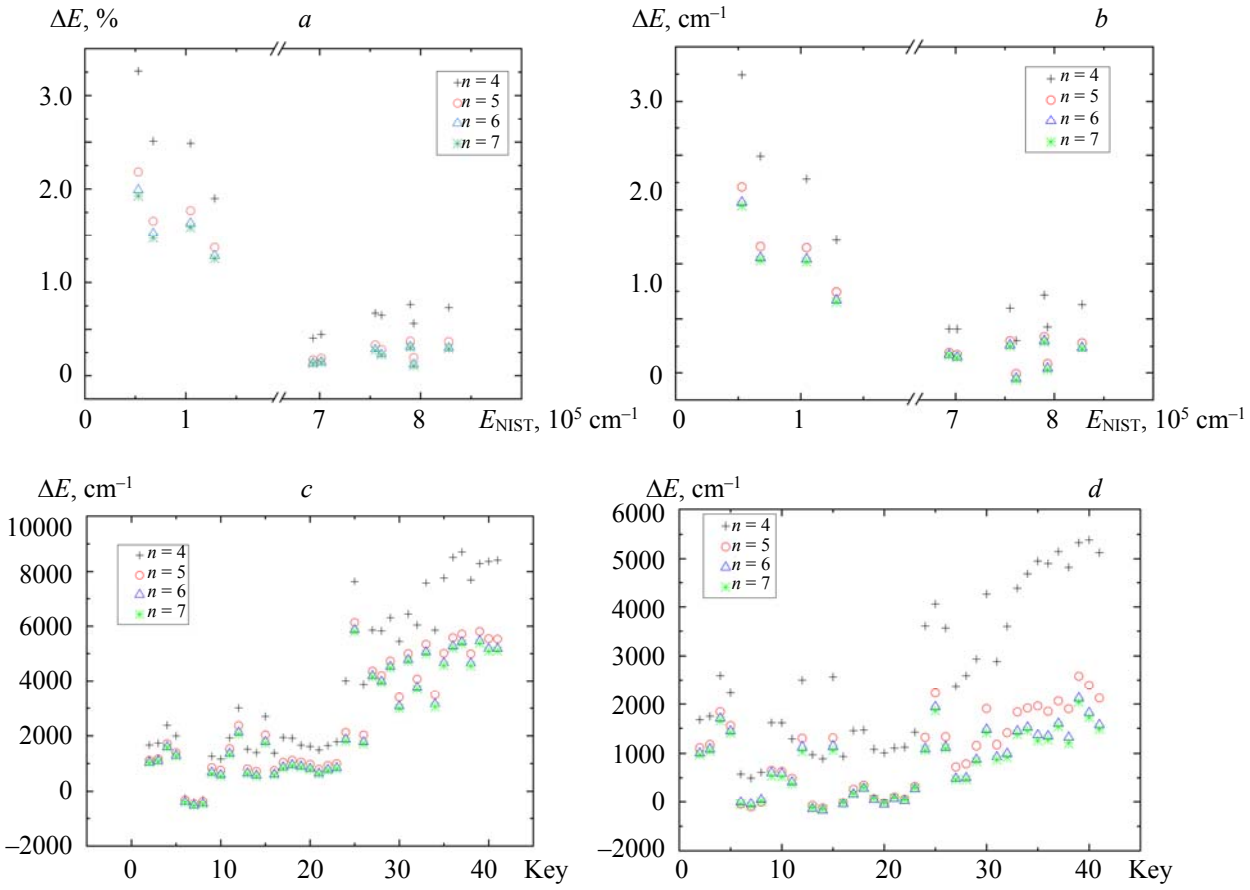

Fig. 1. (a) Energy difference between the core-valence correlation results and the energies for the 11 out of the lowest 41 levels from NIST; (b) Energy difference between the valence-valence correlation results and the energies for the 11 out of the lowest 41 levels from NIST; (c) Energy difference between the valence-valence correlation results and the energies from Vilkas and Ishikawa; (d) Energy difference between the core-valence correlation results and the energies from Vilkas and Ishikawa.

Dirac—Fock wave functions with a minimum number of radial functions are not sufficient to represent the occupied orbitals. Extra configurations have to be added to adequately represent electron correlations (i.e., mixing coefficients) [20]. These extra configurations are represented by CSFs and must have the same angular momentum and parity as the occupied orbitals. The most important contributions to the total wave function of a given level are those from the same configuration [21, 22]. For example, the configuration-mixed wave function for the $3s^23p^3(^4S_{3/2})$ level is represented as $3s^23p^3(^4S_{3/2}) = 0.87\ 3s^23p^3(^4S_{3/2}) + 0.09\ 3s^23p^3(^2P_{3/2})$, where 0.87 and 0.09 are contributions. Clearly, the present VV and CV results are very close to the on-line data from ADAMANT (Table 2), but two levels are different, the first is the level $3s^23p^13d\ ((^3P)^2S_{1/2}) = = 0.23\ 3s^23p^23d\ ((^3P)^2S_{1/2}) + 0.34\ 3s3p^4\ (^2S_{1/2}) + 0.29\ 3s3p^4\ (^2P_{1/2})$ for CV, while $3s^23p^23d\ ((^3P)^2S_{1/2}) = = 0.34\ 3s^23p^23d\ ((^3P)^2S_{1/2}) + 0.29\ 3s3p^4\ (^2S_{1/2}) + 0.23\ 3s3p^4\ (^2P_{1/2})$ for ADAMANT. The second is $3s^23p^23d\ ((^1S)^2D_{5/2}) = 0.23\ 3s^23p^23d\ ((^1S)^2D_{5/2}) + 0.41\ 3s^23p^23d\ ((^3P)^2D_{5/2}) + 0.16\ 3s^23p^23d\ ((^1D)^2D_{5/2})$ for CV, while $3s^23p^23d\ ((^1S)^2D_{5/2}) = 0.39\ 3s^23p^23d\ ((^1S)^2D_{5/2}) + 0.40\ 3s^23p^23d\ ((^3P)^2D_{5/2}) + 0.40\ 3s^23p^23d\ ((^1D)^2D_{5/2})$ for ADAMANT. This is because for more complex system it happens sometimes that two levels have the same dominating *LSJ* term. Then two different levels possess the same quantum label in the represented calculations. For levels 12 and 15, 18 and 23, and 32 and 41, we have this case, and the corresponding term is

adjusted by the main contribution from a procedure JJ2LSJ. Note that the results of Vilkas and Ishikawa [10] and the on-line data from ADAMANT marked the same quantum labels only with a and b. It is necessary to point that the indentation of levels with the same quantum labels should be checked with the experimental results.

TABLE 2. LS-composition (%) for the Lowest 41 Levels in Ga XVII

Key	VV	CV	ADAMANT
1	87 + 9(5)	87 + 9(5)	87 + 8(5)
2	75 + 16(5) + 7(1)	75 + 16(5) + 7(1)	75 + 16(5)
3	97	97	97
4	96	97	96
5	72 + 20(2) + 4(1)	72 + 20(2) + 4(1)	72 + 20(2)
6	86 + 9(27) + 3(10)	86 + 9(27) + 3(10)	86 + 9(27)
7	86 + 10(28)	86 + 10(28)	86 + 10(28)
8	84 + 10(29) + 4(15)	84 + 10(29) + 4(15)	84 + 10(29)
9	70 + 16(33) + 3(11)	70 + 16(33) + 3(11)	70 + 16(33) + 3(11)
10	74 + 17(22) + 4(27)	74 + 17(22) + 4(27)	74 + 17(22)
11	44 + 39(25) + 5(38)	44 + 40(25) + 6(38)	44 + 41(25) + 5(38)
12	24 + 34(15) + 28(31)	23 + 34(15) + 29(31)	34 + 29(15) + 23(31)
13	87 + 5(20) + 3(30)	87 + 5(20) + 3(30)	87 + 5(20)
14	81 + 13(22) + 2(32)	81 + 13(22) + 2(32)	82 + 12(20)
15	42 + 23(12) + 13(31)	42 + 23(12) + 13(31)	42 + 23(12) + 13(31)
16	88 + 8(23)	88 + 8(23)	88 + 12(23)
17	44 + 31(36) + 15(22)	44 + 31(36) + 16(22)	44 + 31(36)
18	34 + 41(23) + 18(37)	34 + 41(23) + 18(37)	41+ 31(23)
19	88 + 6(31) + 2(12)	88 + 6(31)	89 + 5(31)
20	86 + 7(13) + 2(25)	86 + 7(13) + 2(25)	86 + 7(13)
21	90 + 8(26)	90 + 8(26)	90 + 8(26)
22	64 + 12(17) + 10(36)	63 + 12(17) + 10(36)	64 + 12(17) + 10(36)
23	48 + 21(18) + 17(37)	48 + 21(18) + 17(37)	47 + 22(18) + 17(37)
24	88 + 8(18)	87 + 8(18)	88 + 7(18)
25	42 + 22(12) + 19(38)	42 + 23(12) + 19(38)	42 + 24(12) + 19(38)
26	90 + 8(21)	90 + 8(21)	90 + 7(21)
27	78 + 8(6) + 3(32)	78 + 7(6) + 3(32)	79 + 8(6) + 3(32)
28	64 + 8(38) + 8(30)	68 + 8(38) + 8(30)	71 + 8(38) + 7(30)
29	56 + 15(35) + 9(31)	57 + 15(35) + 9(31)	56 + 15(35) + 9(31)
30	34 + 32(40) + 16(28)	36 + 34(40) + 12(28)	38 + 35(40) + 10(28)
31	31 + 25(29) + 19(35)	31 + 24(29) + 19(35)	30 + 25(29) + 19(35)

As for the calculated wavelengths of transition between the lowest 41 levels in Ga XVII, the experimental data compiled by NIST listed the observed wavelengths for eight $E1$ and nine $M1$ transitions. A comparison between the present wavelengths and the NIST and theoretical results [19] is shown in Table 3. The accuracy of the calculated CV wavelengths can be assessed from Table 3, where the agreement is within 0.21 Å for all the available transitions except the 3–37 $3s^23p^3(^2D_{5/2})$–0.34 $3s^23p^23d$ $((^3P)^2F_{7/2})$ one with the calculated wavelength $\lambda = 138.22$ Å and the deviation from the measurement about 0.27 Å. The difference between VV results and the experimental results is in the range –0.44–0.99 Å, while it is in the range –0.41 to –1.09 Å for ADAMANT. It should be noted that the majority of the theoretical results is smaller than the experimental ones. So, another calculation or new measurement is needed to check the results. The wavelengths and transition probabilities for $M1$ transitions are listed in Table 4. The present wavelengths differ from the NIST results by about 0.31–1.14%, while for ADAMANT this difference is 0.11–5.66%. The quoted experimental wavelength uncertainties are about ±25% [23]. So, the deviations actually reflect the estimated errors in wavelengths. The transition probabilities from both theoretical and experimental results are nearly the same, which proves the reliability of the present calculation.

TABLE 3. Comparison between the Present Calculations of $E1$ Wavelengths and the Experimental Data for Eight $E1$ Transitions in Ga XVII

i	j	Wavelengths for $E1$ transitions, Å			
		NIST [18]	VV	CV	ADAMANT [19]
3	37	138.49	137.50	138.22	137.75
2	34	141.16	140.72	141.02	140.57
2	33	142.39	141.47	142.18	141.98
1	28	142.53	141.62	142.32	141.96
5	41	142.97	142.05	142.81	141.88
3	34	144.18	143.71	144.03	143.43
1	27	144.21	143.26	144.02	143.58
4	38	145.22	144.67	145.40	144.75

TABLE 4. Comparison between the Present Calculations of $M1$ Wavelengths (in Å) and the Experimental Data for Nine $M1$ Transitions in Ga XVII

Level		Wavelengths, Å			Transition Probability, s^{-1}		
i	j	NIST	Present	ADAMANT [19]	NIST	Present	ADAMANT [19]
1	5	777.70	768.83	778.61	1.91×10^{3}	2.02×10^{3}	1.95×10^{3}
1	4	955.80	941.42	945.58	1.82×10^{3}	1.94×10^{3}	1.82×10^{3}
2	5	1321.68	1314.64	1346.98	2.76×10^{3}	2.78×10^{3}	2.53×10^{3}
1	3	1476.50	1454.11	1462.80	6.39×10^{2}	7.02×10^{1}	6.42×10^{1}
3	5	1643.40	1631.38	1664.67	7.79×10^{2}	7.79×10^{2}	7.24×10^{2}
1	2	1889.80	1851.79	1845.20	7.64×10^{2}	8.45×10^{2}	7.80×10^{2}
2	4	1934.00	1914.97	1939.45	4.11×10^{2}	4.12×10^{2}	4.00×10^{2}
4	5	4173.00	4193.56	4409.37	9.37×10^{1}	9.10×10^{1}	7.87×10^{2}
2	3	6750.00	6771.17	7058.16	2.65×10^{1}	2.67×10^{1}	2.37×10^{1}

The full set of $E1$, $E2$, $M1$, and $M2$ transitions data can be obtained from the authors by e-mail. The transition rates, line, and oscillator strengths are given in two Coulomb (velocity) and Babushkin (length) gauges. The relative difference (dT) ($dT = \mathrm{abs}(A_l - A_v)/\max(A_l, A_v)$) between the allowed transition rates in length and velocity gauges can be treated as a known accuracy indicator [24]. The closer the dT value is to 0, the greater the precision. In many cases the values are reasonably close to 0 but in other cases, for example the $3s^23p^3\ {}^2D_{5/2}$–$3s^23p^23d$ ($(^1D)^2D_{5/2}$) transition, the difference is up to 0.978. This is because this transition is weak, and the transition probability is only 2.834×10^{6} s^{-1}.

Conclusions. MCDHF and RCI calculations for $3s^23p^2$, $3s3p^3$, and $3s^23p^23d$ configurations of P-like Ga are represented. Fine structure energy levels, oscillator strengths, and transition probabilities for $E1$, $E2$, $M1$, and $M2$ transitions among levels belonging to these levels are performed. The valence-valence and core-valence correlation effects are accounted for in detail. The calculated energy levels and weighted oscillator strengths with a core-valence correlation effect show good agreement with both theoretical and experimental data from the literature. The computed wavelengths are of almost spectroscopic accuracy, aiding line identification in the spectra. Our results are useful for many applications such as controlled thermonuclear fusion, laser and plasma physics, as well as astrophysics.

Acknowledgments. This work was supported by the National Natural Science Foundation of China (11604284).

REFERENCES

1. N. Heidarian, R. E. Irving, S. R. Federman, D. G. Ellis, S. Cheng, L. J. Curtis, *J. Phys. B: At. Mol. Phys*., **50**, 155007 (2017).
2. T. Rauch, K. Werner, P. Quinet, J. W. Kruk, *Astron. Astrophys*., **577**, A6 (2015).
3. B. He, X. J. Meng, J. G. Wang, *Matter Radiat. Extremes*, **1**, 257–263 (2016).

4. K. M. Aggarwal, *At. Data Nucl. Data Tables,* **125**, 226–260 (2019).
5. J. Q. Li, C. Y. Zhang, R. Si, K. Wang, C. Y. Chen, *At. Data Nucl. Data Tables,* **126**, 158–294 (2019).
6. J. Ekman, P. Jönsson, L. Radžiūtė, G. Gaigalas, G. Del Zanna, I. P. Grant, *At. Data Nucl. Data Tables*, **120**, 152–262 (2019).
7. J. Sugar, V. Kaufman, *J. Opt. Soc. Am. B*, **1**, 218–223 (1984).
8. K. N. Huang, *At. Data Nucl. Data Tables*, **30**, 313–421 (1984).
9. E. Charro, I. Martín, M. A. Serna, *J. Phys. B*, **33**, 1753–1766 (2000).
10. M. J. Vilkas, Y. Ishikawa, *J. Phys. B*, **37**, 4763–4778 (2004).
11. E. Träbert, *Atoms,* **2**, 15–85 (2014).
12. P. Jönsson, G. Gaigalas, J. Bieroń, C. F. Fischer, I. P. Grant, *Comput. Phys. Commun.*, **184**, 2197–2203 (2013).
13. C. F. Fischer, G. Gaigalas, P. Jönsson, J. Bieroń, *Comput. Phys. Commun*., **237**, 184–187 (2019).
14. F. Hu, J. M. Yang, C. K. Wang, L. F. Jing, S. B. Chen, G. Jiang, H. Liu, L. H. Hao, *Phys. Rev. A*, **84**, 042506 (2011).
15. F. Hu, G. Jiang, J. M. Yang, C. K. Wang, X. F. Zhao, L. H. Hao, *Eur. Phys. J. D*, **61**, 15–20 (2011).
16. F. Hu, Y. Sun, M. F. Mei, C. C. Sang, *J. Appl. Spectrosc*., **85**, 749–759 (2018).
17. I. P. Grant, *Relativistic Quantum Theory of Atoms and Molecules*, Springer, New York (2007).
18. NIST Atomic Spectra Database, http://physics.nist.gov/PhysRefData/ASD
19. ADAMANT, http://158.129.165.241/db_elev.php?zp=31&ip=16&approach=1
20. J. Gillaspy, *Trapping Highly Charged Ions: Fundamentals and Applications,* Nova Publishers, New York (2001).
21. F. Hu, Y. Sun, M. F. Mei, *Can. J. Phys.*, **95**, 59–64 (2017).
22. G. Gaigalas, C. Froese. Fischer, P. Rynkun, P. Jönsson, *Atoms*, **5**, 6 (2017).
23. T. Shirai, J. Reader, A. E. Kramida, J. Sugar, *J. Phys. Chem. Ref. Data*, **36**, 509–615 (2007).
24. J. Ekman, M. R. Godefroid, H. Hartman, *Atoms*, **2**, 215–224 (2014).